Stent Revascularization Restores Cortical Blood Flow and Reverses Tissue Hypoxia in Atherosclerotic Renal Artery Stenosis, But Fails To Reverse Inflammatory Pathways or GFR

Ahmed Saad, MD[1], **Sandra M.S. Herrmann, MD**[1], **John Crane, BS**[1], **James F Glockner, MD, PhD**[2], **Michael A Mckusick, MD**[2], **Sanjay Misra, MD**[2], **Alfonso Eirin, MD**[1], **Behzad Ebrahimi, MD, PhD**[1], **Lilach O. Lerman, MD, PhD**[1], and **Stephen C. Textor, MD**[1]

[1]Division of Nephrology and Hypertension, Mayo Clinic, Rochester Minnesota

[2]Department of Radiology, Mayo Clinic, Rochester Minnesota

Abstract

Background—Atherosclerotic renal artery stenosis (ARAS) is known to reduce renal blood flow (RBF), glomerular filtration rate (GFR) and amplify kidney hypoxia, but the relationships between these factors and tubulo-interstitial injury in the post-stenotic kidney are poorly understood. The purpose of this study was to examine the effect of renal revascularization in ARAS on renal tissue hypoxia and renal injury.

Methods and Results—Inpatient studies performed in ARAS patients (n = 17), more than 60% occlusion) before and 3 months after stent revascularization, or patients with essential hypertension (EH) (n = 32), during fixed Na+ intake and ACE/ARB Rx. Single-kidney (SK) cortical, medullary perfusion and RBF measured using multidetector CT, and GFR by iothalamate clearance. Tissue deoxyhemoglobin levels (R2*) measured by Blood Oxygen Level Dependent (BOLD) MRI at 3T, as was fractional kidney hypoxia (% of axial area with R2* > 30/s). In addition, we measured renal vein levels of Neutrophil gelatinase-associated lipocalin (NGAL), monocyte chemotactic protein-1 (MCP-1) and Tumor necrosis factor (TNF-α). Pre-stent SK-RBF, perfusion, and GFR were reduced in the post-stenotic kidney. Renal vein NGAL, TNF-α, MCP-1 and fractional hypoxia were higher in untreated ARAS than EH. After stent revascularization, fractional hypoxia fell (p < 0.002) with increased cortical perfusion and blood flow, while GFR and NGAL, MCP-1 and TNF-α remained unchanged.

Conclusions—These data demonstrate that despite reversal of renal hypoxia and partial restoration of RBF after revascularization, inflammatory cytokines and injury biomarkers remained elevated and GFR failed to recover in ARAS. Restoration of vessel patency alone failed to reverse tubulointerstitial damage and partly explains the limited clinical benefit of renal stenting. These results identify potential therapeutic targets for recovery of kidney function in renovascular disease.

Address for Correspondence: Stephen C. Textor, MD, 200 First Street. SW, Rochester, MN, Telephone: 507-284-4083, Fax: 507-266-7891, textor.stephen@mayo.edu.

Disclosures: None.

Atherosclerotic renal artery stenosis (ARAS) produces lumen occlusion, eventually lowering kidney perfusion and accelerating hypertension. ARAS is strongly associated with cardiovascular disease and progressive renal dysfunction [1, 2]. Although the kidneys can adapt to partially reduced blood flow without major loss of oxygenation [3] and viability (as they receive more blood than needed for their metabolic activity), severe reductions in renal blood flow (RBF) eventually lead to tissue fibrosis and what has been labeled " ischemic nephropathy" [4]. Recent experimental studies underscore the development of renal microvascular changes distal to a stenosis in the renal artery [5, 6] and over time, rarefaction of the distal arterioles. Severe degrees of vascular occlusion lead to overt cortical hypoxia [7] associated with fibrogenesis and loss of renal function [8, 9].

The benefits of revascularization procedures to restore blood flow in ARAS remain ambiguous. Only a fraction of patients treated with renal revascularization have improved blood pressure levels or reduced medication requirements, and kidney function after revascularization infrequently improves and sometimes declines[10, 11]. Notably, most clinical studies in humans evaluating the response to revascularization are limited to changes in serum creatinine, GFR, blood pressure, or number of medications [12, 13]. The effects of restoring blood flow after revascularization on kidney tissue hypoxia, regional perfusion within the kidney and markers of renal injury are not known.

Blood oxygen level–dependent (BOLD) MRI has been used to provide estimates of in vivo tissue oxygenation in humans non-invasively by determining local levels of deoxyhemoglobin within the kidney [14-16]. Studies of patients with moderate ARAS during antihypertensive therapy showed remarkably preserved medullary and cortical oxygenation using (BOLD) MRI [3]. Patients with high-grade RAS but with preserved tissue volume demonstrate elevated medullary and cortical deoxyhemoglobin signals that fall after intravenous furosemide [16]. These observations suggest that viable kidneys may show regional hypoxic changes associated with tubular transport activity. When ARAS produces more severe occlusion, overt tissue hypoxia and renal injury can be identified [7, 17]. We have previously shown elevated renal vein levels of neutrophil gelatinase associated lipocalin (NGAL) in the post-stenotic kidney of ARAS patients [18] as well as release of inflammatory markers from the post-stenotic kidney[19]. Whether these inflammatory changes can be reversed in humans remains unknown.

The purpose of this study was to examine the effect of renovascular revascularization on regional tissue perfusion and renal tissue hypoxiain post-stenotic kidneys (STKs) using BOLD magnetic resonance imaging. We sought to evaluate markers of renal injury as reflected by renal vein levels of the acute phase reactant (NGAL), the inflammatory cytokines monocyte chemoattractant protein-1 (MCP-1) and tumor necrosis factor (TNF-) from hypertensive human subjects with ARAS as compared with patients with essential hypertension (EH). Our hypothesis was that restoring blood flow to the stenotic kidney would reverse tissue hypoxia detected by BOLD MR and reduce renal injury in human subjects with ARAS.

Methods

Patient selection

Patients identified with EH (n=32) or ARAS (n=17, scheduled for renal revascularization for clinical indications) seen between January 2008 to September 2012 participated in this study during a 3-day inpatient protocol on two occasions (before and after renal artery revascularization) in the clinical research unit of Saint Mary's Hospital (Rochester, MN), as previously described [20]. Since 4 patients had bilateral stenosis (only one kidney per patient was randomly selected for analysis), and three atrophic kidneys were excluded, 10 non-stenotic (contralateral kidneys (CLK)) were available for analysis. Dietary intake was regulated at 150 mEq of sodium with an isocaloric diet prepared on site. Patients with ARAS were identified using criteria similar to those stipulated for recruitment in the Cardiovascular Outcomes in Renal Atherosclerotic Lesions Trial with cross-sectional luminal occlusion of at least 60% but with the requirement for serum creatinine less than 2.5 mg/dL [21]. Informed, written consent was obtained as approved by the institutional review board of the Mayo Clinic. Severity of renal artery stenosis was estimated by Doppler ultrasound measurements in the affected artery and quantitative vascular imaging using computed tomography (CT) images, as described below. Patients continued previous medications, and all received agents blocking the renin-angiotensin system during these studies (ACE inhibitors or ARBs). ARAS patients returned for repeat measurements 3-4 months after renal revascularization. After the stenting, to exclude any segmental or intra-renal disease, we performed a completion angiogram every time. The angiogram done after the end of the procedure showed patent peripheral arteries without small distal stenoses or occlusion.

Renal function and blood pressure measurements

The first study day included measurement of sodium excretion and of glomerular filtration rate (GFR) by iothalamate clearance (iothalamate meglumine, Conray, Mallinckrodt) after oral hydration (20 mL/kg) over three 30-minute timed collection periods, as described previously[22, 23]. Single kidney GFR was determined by apportioning the measured Iothalamate clearance by percentage of blood flow for each kidney. Blood pressure was measured by automated oscillometric recordings including 3 values taken 3 times daily (an automated oscillometric unit, Omron blood pressure, measured blood pressure at 5, 7, and 9 minutes after a 5-minute rest).

Tissue oxygenation determined by Blood Oxygen Level Dependent (BOLD) MRI

On the second day, BOLD MRI examinations were performed on a GE Twin Speed Signa EXCITE 3.0T system (GE Medical Systems, Waukesha, WI) using a 12-channel torso phased array coil [20]. Three-plane single shot fast spin echo localizers were performed during suspended respiration followed by additional scout images (single shot fast spin echo) oriented parallel to the long axis of each kidney. These long axis scout images were then used to prescribe transverse BOLD images in a plane orthogonal to the long axis. BOLD imaging consisted of a 2D fast spoiled gradient echo sequence with multiple echo times (TEs). Twelve echoes were obtained for each section location, with echo times ranging from 2.5 to 50.0 ms. Imaging parameters for the BOLD acquisition included the following: repetition time (TR) 140 ms, flip angle 45°, section thickness 5 mm, imaging matrix 224×160 to 192, and field of view 32 to 40 cm, with 0.7 to 1.0 partial phase field of view. Image matrix and TR were adjusted in patients with limited breath hold capacity and the field of view and partial field of view adjusted according to patient size. BOLD images were prescribed transverse to the long axis of the kidney using the long axis localizers and acquired during suspended respiration through the midpole hilar region of each kidney. Parametric images of R2* were then generated by fitting signal intensity versus TE data to

an exponential function on a voxel-by-voxel basis and solving for R2* [16]. After the first BOLD acquisition, furosemide (20 mg) was administered intravenously and flushed with 20 mL of saline. BOLD measurements for each kidney were repeated 15 minutes later. Gadolinium-enhanced MR angiograms were obtained after BOLD imaging to confirm the presence or absence of large vessel renal arterial disease. BOLD MRI could not be performed in one patient due to susceptibility artifact from the patient's endovascular aortic aneurysm stent graft.

MRI data analysis

Analysis of BOLD data from axial images was performed by drawing parenchymal regions of interest (ROIs) on 2-4 slices through the midpole hilar region of each kidney on representative T2*-weighted images and then transferring the ROI to the corresponding R2* parametric image. Two ROIs were traced: one which selected the renal cortex (large segment), and a second which included the entire kidney slice, including both cortex and medulla while excluding the renal collecting system and any incidental renal cysts (Figure. 1). MRI BOLD data was processed using Matlab 7.10 (The MathWorks Inc., Natick, MA). To determine the portion of measured kidney area for which tissue hypoxia was present, we defined "fractional tissue hypoxia" by measuring the percentage of voxels from the whole kidney ROI with R2* values above 30 sec^{-1} (mainly represents the medulla) taking the average of all available slices. Previous studies indicate that this value is well above the 95% confidence interval for R2* levels obtained in cortical (non-hypoxic) areas in subjects with either essential hypertension or non-ischemic renovascular disease [7].

Cortical and medullary perfusion and blood flow measured by Multidetector Computerized Tomography (MDCT)

On the third study day, the common femoral vein was cannulated with a 6F sheath and blood samples drawn from the right and left renal veins with a 5F pigtail Cobra catheter (Cook, Inc, Bloomington, IN) for NGAL, MCP-1, and TNF- . The catheter was then advanced into the right atrium for central venous injection of contrast for flow studies using MDCT. MDCT imaging was obtained using a dual-source 64-slice helical MDCT scanner (SOMATOM Definition, Siemens Medical Solutions) after a bolus injection of iopamidol 370 (0.5 mL/kg up to a maximum of 40 mL) using a power injector during respiratory suspension. Perfusion scans were performed at 120 kVp and 160 mAs (adjusted per level of signal-to-noise ratio of the scan) with 20×1.2 collimation and 0 table feed. The flow study was composed of 45 scans, of which the first 35 scans were divided into 3 consecutive scanning sequences (each 20 seconds long), followed by 10 additional scans at 8-seconds intervals. The total scanning time lasted ≈158 seconds, and the longest breath-hold 20 seconds. Images representing 4 slices (5-mm thickness) localized in the hilum region were acquired and reconstructed using a B40f kernel. Fifteen minutes after completion of the perfusion study, a kidney volume study (5-mm thick slices) was performed in the helical mode to determine both cortical and medullary regional volumes.

CT data analysis

MDCT images were reconstructed and displayed with the Analyze™ software package (Biomedical Imaging Resource, Mayo Clinic, MN, USA). Regions of interest (ROI) were selected from cross-sectional images from the aorta, renal cortex, and medulla. Average tissue attenuation in each region was plotted over time and fitted by curve-fitting algorithms to obtain measures of renal function as described previously [24, 25]. Cortical and medullary volumes were calculated by Analyze™ and RBF as the sum of the products of cortical and medullary perfusions and corresponding volumes.

Renal vein and urine sampling

Renal vein blood samples for NGAL and inflammatory cytokine analysis were obtained from the STK renal vein of all patients, as previously described [3, 19]. Samples were stored at −80°C until measurement. Collected samples were centrifuged, and the supernatant was stored. NGAL (ng/mL) was tested by ELISA according to manufacturer's protocol (BioPorto Diagnostics, Cat# KIT 036). Levels of TNF- and MCP-1 were measured by luminex (Millipore, cat No: MPXHCYTO-60K). Signals were read by the Bio-plex 200 systems (BIO-RAD). All measurements were performed by a single investigator blinded to the clinical data.

Statistical analysis

Statistical analysis was performed using JMP software package version 8.0 (SAS Institute Inc., Cary, NC). Results were expressed as mean and standard deviation (SD) or median (interquartile range [IQR]) for quantitative data, as appropriate, or as number (percentage) forqualitative variables.Comparisons between independent groups with essential hypertension or ARAS were performed using two sample t test with unequal variance(or the Wilcoxon rank sum test for skewed data) and a Chi-squared test or Fisher's exact testfor categorical variables as appropriate. Comparisons between stenotic or contralateral kidneys within the same individuals (pre- and post-furosemide) and (before and after revascularization) were performed using paired-t tests (or Wilcoxon signed-rank test for skewed data).No formal correction was made for multiple comparisons, and thus a significance level of 0.05 was accepted. Spearman rank correlation analysis was used to test for associations between basal fractional hypoxia, inflammatory markers and RBF, tissue perfusion and GFR.

Results

Demographic comparison between ARAS and EH patients

Complete data were available for 17 patients in the ARAS group and 32 EH patients. The demographic and clinical features of the patients studied are summarized in (Table. 1). Age, weight, body mass index (BMI) and most biochemical values were not significantly different between groups. Triglyceride levels, serum creatinine and systolic blood pressure were higher in patients with ARAS, while GFR was lower.

Reduced RBF in ARAS STKs improved after revascularization, while GFR remained reduced

Results from quantitative MDCT measurements of hemodynamics of individual kidneys are summarized in (Table 2). The total volume of post-stenotic kidneys was reduced, primarily due to reduction in cortical volume as compared to EH kidneys but 3 months after technically successful stent revascularization, total kidney volume increased (p = 0.01). Both cortical and medullary perfusions (flow per unit tissue volume) were reduced in the STK compared to kidneys from EH (p = 0.001 and p = 0.03). Measurements after renal artery stenting demonstrated increased cortical (p = 0.01) but not medullary perfusion. Whole kidney blood flow was reduced in the STK as compared to EH kidney (p = 0.001), with partial restoration after revascularization (p = 0.02). Single kidney iothalamate GFR (mL/ min per kidney) in STKs was lower than EH kidneys (p = 0.0009), did not change after stent revascularization (p = 0.12).

Renal revascularization reduced elevated levels of fractional kidney hypoxia in ARAS

Tissue oxygenation levels defined both by R2* values and fractional hypoxia (R2*>30 sec-1), are summarized in (Table 3). Pre-stenting basal and post furosemide fractional

hypoxia levels were higher in STK than EH kidneys as illustrated in (Figure. 2). Fractional tissue hypoxia fell after furosemide administration, but remained above those of essential hypertension. The fractional hypoxia levels in the stenotic kidneys fell to near normal levels when remeasured three to four months after renal artery stenting (Figure. 3A). The fractional hypoxia basal levels correlated inversely with GFR (Spearman rank correlation coefficient r = − 0.38, p = 0.007), RBF (r = − 0.4, p = 0.005) and also with cortical/medullary perfusion (r = − 0.4, p = 0.004).

Representative axial BOLD images (R2* parametric maps) illustrating the change in hypoxia in ARAS kidney before and after revascularization are illustrated in (Figure. 3B).

ARAS was associated with elevated markers of renal inflammation, which persisted after revascularization

Renal vein basal levels of NGAL, MCP-1 and TNF- were elevated in ARAS compared to EH (p = 0.0006, 0.005 and 0.0003, respectively) (Table 4). These venous levels remained unchanged 3 months after revascularization (Figure 4). Levels of renal vein NGAL correlated inversely with GFR (r = − 0.45; p = 0.009). Also MCP-1 (r = − 0.4; p = 0.007) and TNF- correlated inversely with GFR (r = − 0.6; p <0.0001).

The statin therapy, a potential anti-inflammatory, showed no consistent effects on the inflammation markers, RBF, R2* and GFR on this studied cohort (both in RAS and EH). (Supplemental Table 1)

Discussion

This study demonstrates, for the first time, the effect of renal revascularization to reduce the fractions of kidney parenchyma that were measurably hypoxic as a result of reduced blood flow. Cortical blood flows and perfusion were reduced in the post-stenotic kidney and rose after technically successful revascularization, although medullary flows remained below those of EH or the non-stenotic contralateral kidneys (CLK). Hence, the levels of overall fractional tissue hypoxia were reversed by restoring blood flow in the STK. Despite these changes, no consistent changes in single kidney filtration (GFR) or renal venous levels of NGAL, MCP-1 or TNF- in ARAS were identified. These markers of inflammatory renal injury remained elevated above those of essential hypertension and were not affected by restoring blood flow or tissue oxygenation in these patients.

Pre-stenting measurements in our patients using fractional tissue hypoxia confirmed that the stenotic kidneys, but not the non-stenotic CLK from the same patients, indeed were functioning under hypoxic conditions (Table 3). Our results obtained after successful revascularization extend these observations to demonstrate reversal of tissue hypoxia associated with partial restoration of cortical and renal blood flows. Hence, our study underscores the role of renal revascularization to restore tissue oxygenation in the ischemic kidney.

Importantly, restoring blood flow and restoring more normal levels of tissue oxygenation was not associated with reversal of tissue injury markers, as defined by renal venous levels of NGAL, MCP-1 and TNF- . Measured levels of single-kidney GFR did not change in the post-stenotic kidney in these patients and combined GFR for both kidneys remained below those of essential hypertension. Our results extend the results observed in experimental swine models of ARAS that demonstrate microvascular rarefication, oxidative stress injury and interstitial fibrosis within the post-stenotic kidney parenchyma [26]. These results are consistent with increased renal inflammation in ARAS patients, as evidenced by high levels of NGAL (which is an acute phase protein induced in inflammatory conditions and acute

ischemic injury, often used as a biomarker for acute kidney injury [27, 28]) and proinflammatory cytokines TNF- and MCP-1. MCP-1 is an inflammatory cytokine known to recruit macrophages to the kidney [29]. We have recently shown that TGF- expression associated with macrophage infiltration within the human kidney with ARAS is higher than normal kidneys (28) and that renal vein levels of inflammatory cytokines like (IL-6, IF-Y, E selectins and others) are elevated in human ARAS (29). Studies using murine models of renal artery stenosis demonstrate early and sustained activation of TGF- in both the stenotic and contralateral kidney as kidney injury develops [30]. Smad3-knock-out models that eliminate downstream effects of TGF- appear to protect the post-stenotic kidney from injury from reduced blood flow [31]. We interpret all of these data to suggest activation of multiple inflammatory injury pathways in post-stenotic kidneys. Although several of these are recognized to be triggered by tissue hypoxia [32], it is equally clear from the results of our study that removing the hypoxic stimulus failed to reverse this process once it has been established.

Perhaps relevant is the observation that reperfusion by percutaneous angioplasty (PTRA) in swine model of ARAS increases cytokine levels (MCP-1) over several hours, and is associated 4 weeks later with multiple markers of inflammatory injury, oxidative stress, apoptosis, and interstitial fibrosis [33]. These data suggest that inflammatory signals related to reperfusion procedures may participate in activating intracellular or mitochondrial stress injury. We cannot exclude a role for atheroembolic injury associated with renal artery stenting, although no clinical signs were evident in these patients. Our data provide further insights into human treatment trials related to recovery of renal function after revascularization. Although some patients recover some portion of reduced GFR after renal artery stenting, the majority either has no evident change or progress to further loss[11]. As a result, average values for GFR do not change after successful revascularization [34], despite technical success of restoring blood flow. Hence, prospective trials, including The Angioplasty and Stenting for Renal Artery Lesions (ASTRAL) and Stent Placement in Patients With Atherosclerotic Renal Artery Stenosis and Impaired Renal Function (STAR), up to now fail to demonstrate major benefits of restoring blood flow alone to alter the course of renal injury in human ARAS [11, 35].

The present study provides evidence that although advanced renovascular disease does indeed lead to renal tissue hypoxia, restoring blood flow and reversing hypoxia alone regularly failed to alter local inflammatory signals reflecting active processes of tissue injury and inflammation. These data suggest that additional measures that may abrogate those pathways may be essential to halt the progression of injury and perhaps allow repair of functional renal structures. Recent experimental studies using endothelial progenitor cells [36-38] or intra-renal infusion of mesenchymal stem cells indicate that recovery of renal microvessels, blood flow and glomerular filtration is possible in the post-stenotickidney [39]. Additional maneuvers targeting mitochondria at the time of restoring blood flow offer the potential to protect the post-stenotic kidney from reperfusion damage [33].

This study has limitations. It was not a randomized study, but enrolled patients selected for revascularization based on clinical criteria. Most of the patients were males. Our control group was comprised of subjects with EH of similar age, rather than "normal" individuals. The EH group did include some healthy individuals with normal kidney hemodynamics and function. Individuals with ARAS had lower GFR, although most had relatively preserved function and were limited to r serum creatinine levels below 2.5 mg/dL. Diabetic subjects were specifically excluded.

Conclusion

Our results indicate that renal revascularization partially restored cortical and renal blood flows and reversed regional tissue hypoxia within the post-stenotic kidneys. Despite improving blood flow, single kidney GFR did not recover nor did markers of tubulo-interstitial injury (NGAL) and inflammatory cytokines change. These data underscore the importance of ongoing inflammatory and profibrotic injury that revascularization alone fails to reverse in patients with ARAS. They demonstrate the urgent need to identify and develop supplemental management strategies to restore kidney structure and function for patients with vascular occlusive disease.

Supplementary Material

Refer to Web version on PubMed Central for supplementary material.

Acknowledgments

References

1. Kalra P, Guo H, Kausz AT, Gilbertson DT, Liu J, Chen SC, Ishani A, Collins AJ, Foley RN. Atherosclerotic renovascular disease in united states patients aged 67 years or older: Risk factors, revascularization, and prognosis. Kidney Int. 2005; 68:293–301. [PubMed: 15954920]

2. Edwards MS, Craven TE, Burke GL, Dean RH, Hansen KJ. Renovascular disease and the risk of adverse coronary events in the elderly: A prospective, population-based study. Arch Intern Med. 2005; 165:207–213. [PubMed: 15668368]

3. Gloviczki ML, Glockner JF, Lerman LO, McKusick MA, Misra S, Grande JP, Textor SC. Preserved oxygenation despite reduced blood flow in poststenotic kidneys in human atherosclerotic renal artery stenosis. Hypertension. 2010; 55:961–966. [PubMed: 20194303]

4. Garovic VD, Textor SC. Renovascular hypertension and ischemic nephropathy. Circulation. 2005; 112:1362–1374. [PubMed: 16129817]

5. Feltrin GP, Rossi G, Talenti E, Pessina AC, Miotto D, Thiene G, Dal Palu C. Prognostic value of nephrography in atherosclerotic occlusion of the renal artery. Hypertension. 1986; 8:962–964. [PubMed: 3759229]

6. Zhu XY, Chade AR, Rodriguez-Porcel M, Bentley MD, Ritman EL, Lerman A, Lerman LO. Cortical microvascular remodeling in the stenotic kidney: Role of increased oxidative stress. Arterioscler Thromb Vasc Biol. 2004; 24:1854–1859. [PubMed: 15308558]

7. Gloviczki ML, Lerman LO, Textor SC. Blood oxygen level-dependent (bold) mri in renovascular hypertension. Curr Hypertens Rep. 2011; 13:370–377. [PubMed: 21833688]

8. Chade AR, Rodriguez-Porcel M, Grande JP, Krier JD, Lerman A, Romero JC, Napoli C, Lerman LO. Distinct renal injury in early atherosclerosis and renovascular disease. Circulation. 2002; 106:1165–1171. [PubMed: 12196346]

9. Chade AR, Krier JD, Rodriguez-Porcel M, Breen JF, McKusick MA, Lerman A, Lerman LO. Comparison of acute and chronic antioxidant interventions in experimental renovascular disease. Am J Physiol Renal Physiol. 2004; 286:F1079–1086. [PubMed: 14722019]

10. Safian RD, Madder RD. Refining the approach to renal artery revascularization. JACC Cardiovasc Interv. 2009; 2:161–174. [PubMed: 19463421]

11. Wheatley K, Ives N, Gray R, Kalra PA, Moss JG, Baigent C, Carr S, Chalmers N, Eadington D, Hamilton G, Lipkin G, Nicholson A, Scoble J. Revascularization versus medical therapy for renal-artery stenosis. N Engl J Med. 2009; 361:1953–1962. [PubMed: 19907042]

12. Dubel GJ, Murphy TP. The role of percutaneous revascularization for renal artery stenosis. Vasc Med. 2008; 13:141–156. [PubMed: 18593803]

13. Textor SC. Ischemic nephropathy: Where are we now? J Am Soc Nephrol. 2004; 15:1974–1982. [PubMed: 15284283]

14. Prasad PV, Edelman RR, Epstein FH. Noninvasive evaluation of intrarenal oxygenation with bold mri. Circulation. 1996; 94:3271–3275. [PubMed: 8989140]

15. Pedersen M, Dissing TH, Morkenborg J, Stodkilde-Jorgensen H, Hansen LH, Pedersen LB, Grenier N, Frokiaer J. Validation of quantitative bold mri measurements in kidney: Application to unilateral ureteral obstruction. Kidney Int. 2005; 67:2305–2312. [PubMed: 15882272]

16. Textor SC, Glockner JF, Lerman LO, Misra S, McKusick MA, Riederer SJ, Grande JP, Gomez SI, Romero JC. The use of magnetic resonance to evaluate tissue oxygenation in renal artery stenosis. J Am Soc Nephrol. 2008; 19:780–788. [PubMed: 18287564]

17. Lerman LO, Textor SC, Grande JP. Mechanisms of tissue injury in renal artery stenosis: Ischemia and beyond. Prog Cardiovasc Dis. 2009; 52:196–203. [PubMed: 19917330]

18. Eirin A, Gloviczki ML, Tang H, Rule AD, Woollard JR, Lerman A, Textor SC, Lerman LO. Chronic renovascular hypertension is associated with elevated levels of neutrophil gelatinase-associated lipocalin. Nephrol Dial Transplant. 2012; 27:4153–4161. [PubMed: 22923545]

19. Eirin A, Gloviczki ML, Tang H, Gossl M, Jordan KL, Woollard JR, Lerman A, Grande JP, Textor SC, Lerman LO. Inflammatory and injury signals released from the post-stenotic human kidney. Eur Heart J. 2013; 34:540–548a. [PubMed: 22771675]

20. Gloviczki ML, Glockner J, Gomez SI, Romero JC, Lerman LO, McKusick M, Textor SC. Comparison of 1.5 and 3 t bold mr to study oxygenation of kidney cortex and medulla in human renovascular disease. Invest Radiol. 2009; 44:566–571. [PubMed: 19668000]

21. Murphy TP, Cooper CJ, Dworkin LD, Henrich WL, Rundback JH, Matsumoto AH, Jamerson KA, D'Agostino RB. The cardiovascular outcomes with renal atherosclerotic lesions (coral) study: Rationale and methods. J Vasc Interv Radiol. 2005; 16:1295–1300. [PubMed: 16221898]

22. Textor SC, Turner ST. Renal vascular response to sodium loading in sons of hypertensive parents. Hypertension. 1991; 17:982–988. [PubMed: 2045180]

23. Wilson DM, Bergert JH, Larson TS, Liedtke RR. Gfr determined by nonradiolabeled iothalamate using capillary electrophoresis. Am J Kidney Dis. 1997; 30:646–652. [PubMed: 9370179]

24. Lerman LO, Taler SJ, Textor SC, Sheedy PF 2nd, Stanson AW, Romero JC. Computed tomography-derived intrarenal blood flow in renovascular and essential hypertension. Kidney Int. 1996; 49:846–854. [PubMed: 8648929]

25. Daghini E, Primak AN, Chade AR, Krier JD, Zhu XY, Ritman EL, McCollough CH, Lerman LO. Assessment of renal hemodynamics and function in pigs with 64-section multidetector ct: Comparison with electron-beam ct. Radiology. 2007; 243:405–412. [PubMed: 17456868]

26. Eirin A, Zhu XY, Urbieta-Caceres VH, Grande JP, Lerman A, Textor SC, Lerman LO. Persistent kidney dysfunction in swine renal artery stenosis correlates with outer cortical microvascular remodeling. Am J Physiol Renal Physiol. 2011; 300:F1394–1401. [PubMed: 21367913]

27. Mishra J, Dent C, Tarabishi R, Mitsnefes MM, Ma Q, Kelly C, Ruff SM, Zahedi K, Shao M, Bean J, Mori K, Barasch J, Devarajan P. Neutrophil gelatinase-associated lipocalin (ngal) as a biomarker for acute renal injury after cardiac surgery. Lancet. 2005; 365:1231–1238. [PubMed: 15811456]

28. Hirsch R, Dent C, Pfriem H, Allen J, Beekman RH 3rd, Ma Q, Dastrala S, Bennett M, Mitsnefes M, Devarajan P. Ngal is an early predictive biomarker of contrast-induced nephropathy in children. Pediatr Nephrol. 2007; 22:2089–2095. [PubMed: 17874137]

29. Deshmane SL, Kremlev S, Amini S, Sawaya BE. Monocyte chemoattractant protein-1 (mcp-1): An overview. J Interferon Cytokine Res. 2009; 29:313–326. [PubMed: 19441883]

30. Cheng J, Zhou W, Warner GM, Knudsen BE, Garovic VD, Gray CE, Lerman LO, Platt JL, Romero JC, Textor SC, Nath KA, Grande JP. Temporal analysis of signaling pathways activated in a murine model of two-kidney, one-clip hypertension. Am J Physiol Renal Physiol. 2009; 297:F1055–1068. [PubMed: 19625373]

31. Warner GM, Cheng J, Knudsen BE, Gray CE, Deibel A, Juskewitch JE, Lerman LO, Textor SC, Nath KA, Grande JP. Genetic deficiency of smad3 protects the kidneys from atrophy and

interstitial fibrosis in 2k1c hypertension. Am J Physiol Renal Physiol. 2012; 302:F1455–1464. [PubMed: 22378822]

32. Fine LG, Norman JT. Chronic hypoxia as a mechanism of progression of chronic kidney diseases: From hypothesis to novel therapeutics. Kidney Int. 2008; 74:867–872. [PubMed: 18633339]

33. Eirin A, Li Z, Zhang X, Krier JD, Woollard JR, Zhu XY, Tang H, Herrmann SM, Lerman A, Textor SC, Lerman LO. A mitochondrial permeability transition pore inhibitor improves renal outcomes after revascularization in experimental atherosclerotic renal artery stenosis. Hypertension. 2012; 60:1242–1249. [PubMed: 23045468]

34. Textor SC, Misra S, Oderich GS. Percutaneous revascularization for ischemic nephropathy: The past, present, and future. Kidney Int. 2013; 83:28–40. [PubMed: 23151953]

35. Bax L, Woittiez AJ, Kouwenberg HJ, Mali WP, Buskens E, Beek FJ, Braam B, Huysmans FT, Schultze Kool LJ, Rutten MJ, Doorenbos CJ, Aarts JC, Rabelink TJ, Plouin PF, Raynaud A, van Montfrans GA, Reekers JA, van den Meiracker AH, Pattynama PM, van de Ven PJ, Vroegindeweij D, Kroon AA, de Haan MW, Postma CT, Beutler JJ. Stent placement in patients with atherosclerotic renal artery stenosis and impaired renal function: A randomized trial. Ann Intern Med. 2009; 150:840–848. W150–841. [PubMed: 19414832]

36. Ebrahimi B, Li Z, Eirin A, Zhu XY, Textor SC, Lerman LO. Addition of endothelial progenitor cells to renal revascularization restores medullary tubular oxygen consumption in swine renal artery stenosis. Am J Physiol Renal Physiol. 2012; 302:F1478–1485. [PubMed: 22419692]

37. Chade AR, Zhu X, Lavi R, Krier JD, Pislaru S, Simari RD, Napoli C, Lerman A, Lerman LO. Endothelial progenitor cells restore renal function in chronic experimental renovascular disease. Circulation. 2009; 119:547–557. [PubMed: 19153272]

38. Chade AR, Zhu XY, Krier JD, Jordan KL, Textor SC, Grande JP, Lerman A, Lerman LO. Endothelial progenitor cells homing and renal repair in experimental renovascular disease. Stem Cells. 2010; 28:1039–1047. [PubMed: 20506499]

39. Eirin A, Zhu XY, Krier JD, Tang H, Jordan KL, Grande JP, Lerman A, Textor SC, Lerman LO. Adipose tissue-derived mesenchymal stem cells improve revascularization outcomes to restore renal function in swine atherosclerotic renal artery stenosis. Stem Cells. 2012; 30:1030–1041. [PubMed: 22290832]
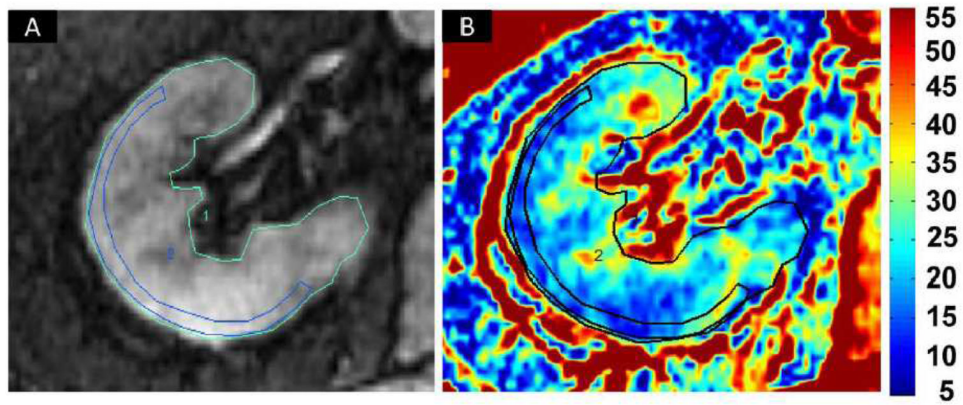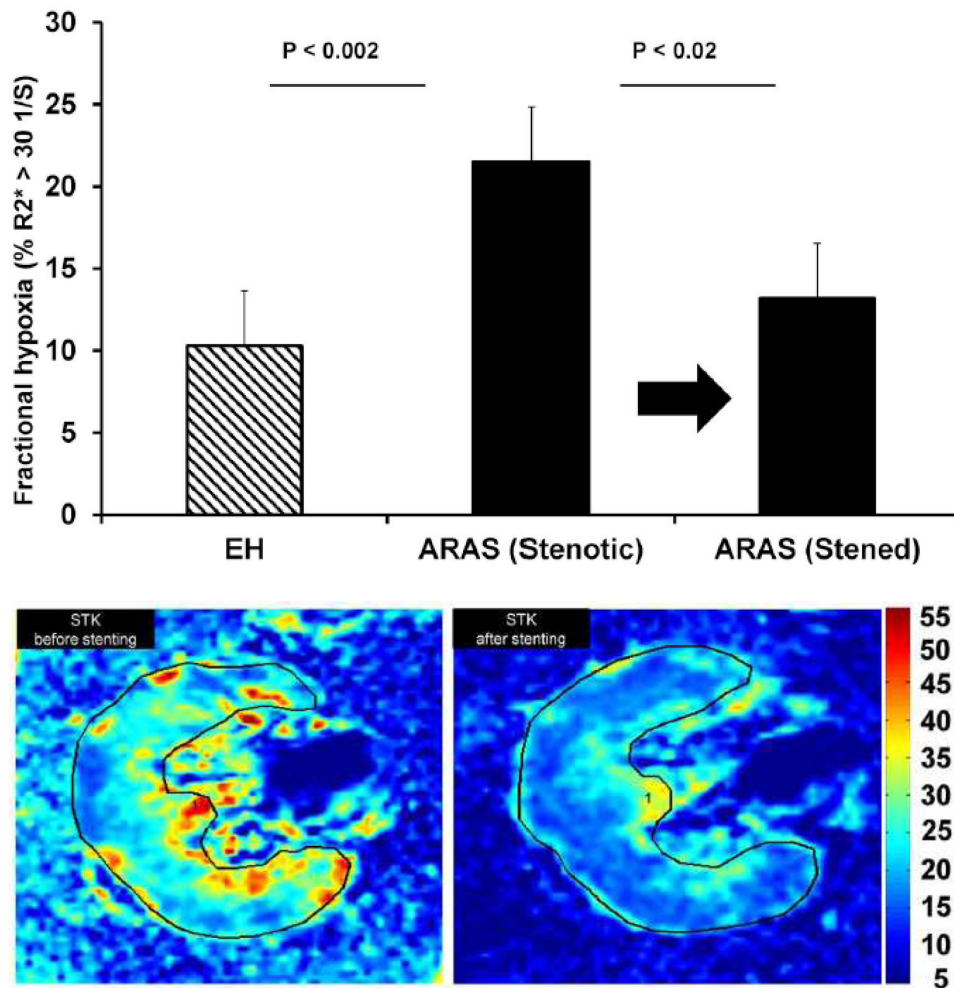
Figure 1.
Blood Oxygen Level Dependent (BOLD) MR: Selection of regions of interest (ROI) on an axial image: (A) Fractional tissue hypoxia was determined by outlining the entire axial kidney slice located within parenchyma. An additional ROI was placed to outline a "wide segment" cortical area excluding the renal collecting system, incidental cysts and the hilar vessels. (B) R2* parametric map for the selected axial slice reflecting widely variable R2* levels and deoxyhemoglobin at different sites within the kidney, particularly in medullary zones. This method of BOLD analysis bypasses observer selection of specific ROIs in the medulla and allows estimation of the fraction of the entire slice that exceeds the threshold above 30 sec^{-1} (see text).
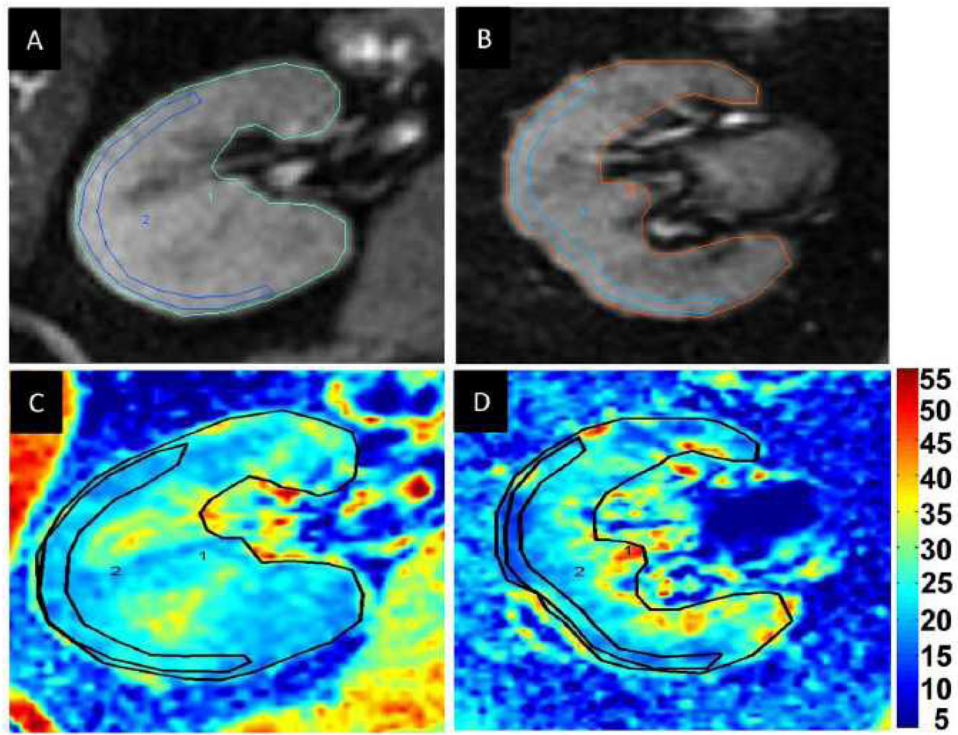
Figure 2.
A,B,C and D: Examples of T2* images and R2* parametric maps for a subject with essential hypertension (A and C) and a subject with ARAS (B and D) obtained using the same color scale for R2*. Fractional hypoxia above 30 sec^{-1} in ARAS was greater than in EH (28.5 vs 11.3 %)
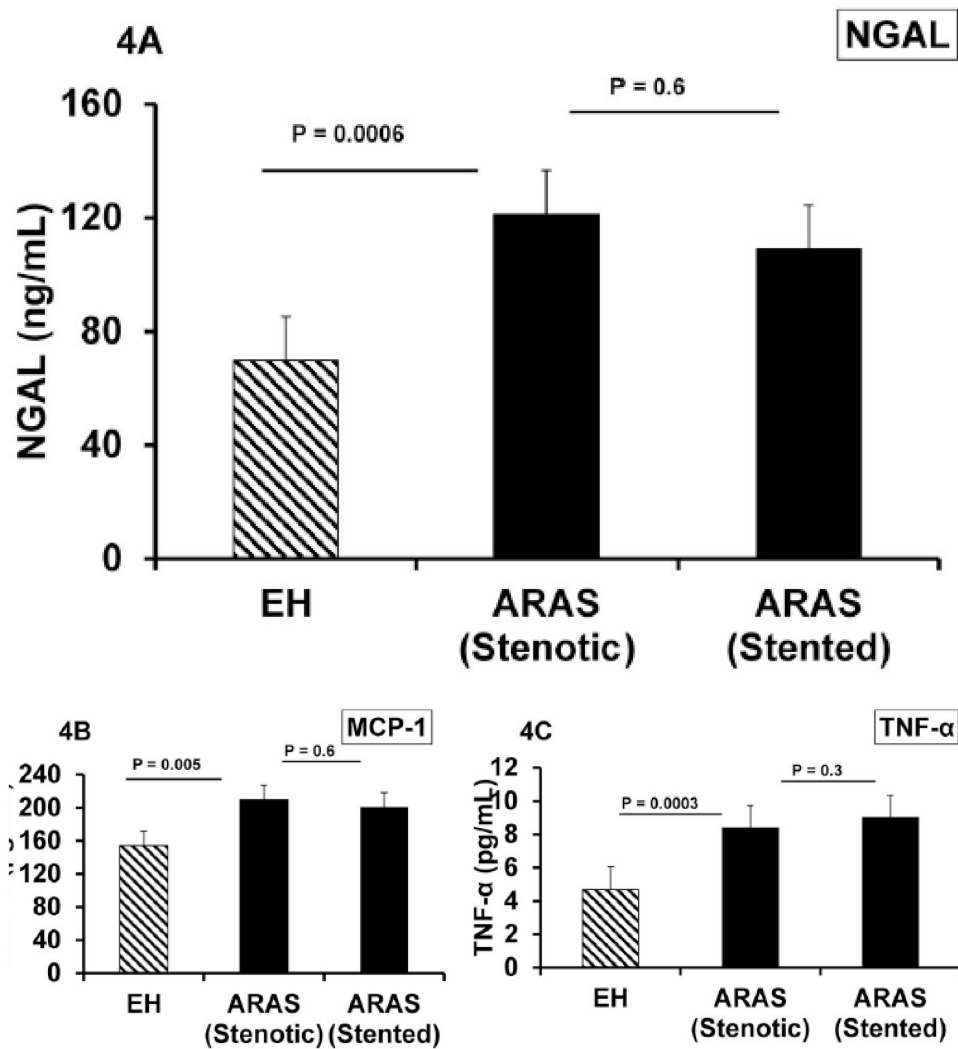
Figure 3.
A. Changes in tissue oxygenation after renal revascularization:
Mean Fractional hypoxia levels in STK were higher compared to EH (P < 0.002). Hypoxia levels fell significantly after stent revascularization (P = 0.02)
B. Individual example of Axial BOLD images (R2* parametric maps depicting effects of deoxyhemoglobin) illustrating the change in hypoxia in ARAS kidney before and after revascularization (Left and right). There were lower R2* levels associated with hypoxia after stenting in both the cortical and medullary regions.

Figure 4.
Renal vein levels of NGAL, MCP-1 and TNF- (A, B and C) were higher in ARAS compared to essential hypertension and remained unchanged 3 months after revascularization. Despite increased cortical blood flow and tissue perfusion and reversal of tissue hypoxia, renal venous markers of tubulo-interstitial injury and inflammatory cytokines were persistently elevated.

Table 1

Clinical, laboratory, and demographic data of EH and ARAS patients

	EH (N=32)	ARAS (N=17)	P value
Gender (% Male)[*]	59	76	0.35
Age (years)	63.1 ± 16.3	68 ± 8.8	0.17
Creatinine (mg/dl)	0.96 ± 0.26	1.4 ± 0.4	0.0004
Iothalamate clearance GFR (mL/min)	87.9 ± 24.3	65.6 ± 31.9	0.01
ACE or ARBs (Yes/No) [*]	31 / 1	17 / 0	1.01
Statins (yes %)[*]	16 (50%)	12 (71%)	0.23[*]
Number of anti-HTN drugs[#]	3 (2, 4)	3 (2.5, 4.5)	0.19
SBP(mmHg)	135 ±19	147 ± 20	0.04
DBP (mmHg)	71 ± 12	71 ± 11.4	0.87
Weight (kg)	78.3 ± 15.6	86 ± 18	0.14
BMI (kg/m2)	27.3 ± 4.3	28.6 ± 3.9	0.19
Hematocrit %	40.3 ± 4	38 ± 3.7	0.06
Total Cholesterol (mg/dl)	182 ± 30	181.2 ± 36.2	0.97
TG (mg/dl)	130.6 ± 58	184 ± 95.6	0.04
HDL (mg/dl)	52.3 ± 12	45.6 ± 21	0.30
LDL (mg/dl)	103 ± 23	98.6 ± 28	0.57
Microalbumin(mg/24h)[#]	19 (13, 29)	19.5 (10.3, 42.5)	0.69

Mean±SD, GFR=glomerular filtration rate, Anti-HTN=antihypertensive, ACEI=angiotensin converting enzyme inhibitors, ARB=angiotensin receptors blockers, SBP=systolic blood pressure, DBP=diastolic blood pressure, ARAS= atherosclerotic Renal artery stenosis, EH=essential hypertension, N= number of patients.

[#]Median (IQR) reported due to skewed data, P value obtained from Wilcoxon rank sum test;

[*]Fisher's exact test.

Table 2

Multidetector CT Measurements of individual kidney volume, tissue perfusion, blood flow and iothalamate filtration

Single Kidney	EH (N=32)	STK (N=17) Baseline	STK (N=17) 3 months	CLK (N=10) baseline	CLK (N=10) 3 months
Total kidney volume (CT), mL	145.9±36	123.9 ± 45.3 *	137.7 ± 48.5 †	175 ± 52 †§	162.4 ± 59.9
Cortical volume, mL	96.7±29	78.6 ± 37.1 *	86.7 ± 36	109 ± 44 §	111 ± 47
Medullary volume, mL	49±14.6	45.3 ± 16.7	51 ± 17	66 ± 24 †§§	51.4 ± 17.7
Cortical perfusion, mL/min per mL of tissue	3.4±0.99	2.3 ± 0.4 *	2.7 ± 0.6 †	2.9 ± 0.4 §	2.6 ± 0.9
Medullary perfusion, mL/min per mL of tissue	1.3±0.48	1.06 ± 0.2 *	1.01±0.29	1.13 ± 0.3	1.06 ± 0.5
Total renal blood flow, mL/min	399±174	238.3 ± 119 *	296.5 ± 174 †	398 ± 162 §	372.3 ± 221
Cortical flow, mL/min	331±161	189.3 ± 102 *	242.9 ± 149 †	325 ± 153 §	313.9 ± 195
Medullary flow, mL/min	63±25	49 ± 25 *	53.5 ± 31	73.8 ± 36.7	58.4 ± 39.7
Single kidney GFR, mL/min per kidney	44.3±13.5	28.3 ± 15.5 *	32.6 ± 19.1	47.9 ± 21.8 §	40.5 ± 21.2

EH: essential hypertension, STK: stenotic kidney, CLK: contralateral kidney

*
P<0.05 vs. EH,

†
p< 0.05 vs STK–baseline,

†
p<0.05 vs.EH,

§
p<0.05 vs. STK baseline,

#
p< 0.05 vs. CLK baseline.

Table 3

BOLD MRI for Essential Hypertension and Atherosclerotic Renal Artery Stenosis before and after revascularization using Fractional Tissue Hypoxia and Cortical regions of interest (ROI) measurements

Single Kidney		EH (N=32)	STK (N=17)		CLK (N=10)	
			Baseline	*3 months*	*baseline*	*3 months*
Fractional Hypoxia (% R2 * > 30 sec^{-1})	Pre-furosemide	8.7(3.5,13.3)$^{\#}$	19.2(9.2,28.3)$^{*\#}$	11.5(5.5,16.5)$^{\#}$†	14.3(3.7,15.4)$^{\#}$	9.3 (4.6, 20)$^{\#}$
	Post-furosemide	2.6(1.35,6.4)$^{\#\$}$	12.5 (3,21.5)$^{*\#\$}$	5.2 (2.5,12.6)$^{\#}$†$^{\$}$	5.6 (2.6, 10)$^{\#}$	3.5(1.5,14.6)$^{\#\$}$
Cortex R2 * (sec^{-1})	Pre-furosemide	18.5 ± 2.7	21 ±4.4	19.7 ± 2.6	18±2.3	19.3±2.8
	Post-furosemide	16.7 ± 2.2$^{\$}$	19.5 ± 4.6$^{*\$}$	18.2±2$^{\$}$	17.6±3.9	18±2.7$^{\$}$

Data are Mean±SD.

$^{\#}$Median (IQR) reported due to skewed data (P value derived from Wilcoxon rank sum test or from Wilcoxon signed-rank test as appropriate).

*P<0.05 vs. EH.

†p< 0.05 vs STK-baseline.

†p<0.05 vs.EH.

$^{\$}$p<0.001 pre (furosemide) vs post (furosemide).

Table 4

Renal vein levels of NGAL, MCP-1 and TNF-

	EH	STK-Baseline	P vs. EH	STK-3 months	P vs. baseline
MCP-1 (pg/mL)	154 ± 71	208.2 ± 83	0.005	200 ± 93.6	0.6
TNF- (pg/mL)	4.7 ± 4.2	8.4 ± 5.8	0.0003	9 ± 5.8	0.3
NGAL (ng/mL)	69.7 ± 36.5	121.2 ± 55	0.0006	108.8 ± 35	0.6

EH: essential hypertension, STK: stenotic kidney